Adaptive Robust Control for Flexible Manipulators

Jung-Hua Yang[1] & Feng-Li Lian[1] & Li-Chen Fu[1,2]
1. Lab. 205, Department of Electrical Engineering
2. Department of Computer Science and Information Engineering
National Taiwan University, Taipei, Taiwan, R.O.C.

Abstract

Because the control D.O.F. (Degree of Freedom) is much fewer than the motion D.O.F. when a flexible manipulator is commanded to track a desired trajectory , many control strategies that succeed in conventional rigid-robot control cannot be directly applied to solve the flexible robot control problem. In this work, an adaptive variable structure scheme has been proposed to solve such a problem. The full nonlinear dynamics of the whole system are all taken into account for the control design. To alleviate the chattering phenomenon commonly seen in variable structure type of control, a saturation type adaptive scheme has also been proposed. For verification of the effectiveness of the proposed controller, a two-link flexible manipulator is built up and the promise of the controller is experimentally demonstrated.

1 Introduction

In the recent years, much attention has been paid to the modeling and control of robotic manipulators with flexible links. For high structural stiffness, conventional rigid robots are often built to be heavy and bulky. Accordingly, some drawbacks, such as high power-consumption, low motion speed, actuators with high capacity, and low payload ratio, may appear. To remedy these problems, the links of a manipulator are made lighter. Therefore, the structural flexibility can no longer be ignored, especially when the motion speed of the robot is high.

In the literature, there have been many control schemes proposed for flexible manipulators. In [1], [2], linear system approaches were used to control a single-link flexible robot. In there, LQG and the stable factorization technique have been used for the control design. Differently, Yurkovitch et al. [5], [6], used acceleration feedback for the end-point position control of a flexible robot arm. These results have been compared with those obtained by using LQG approach, and better performance has been shown. To overcome the modeling uncertainty, in [3], [4], some self-tuning type adaptive control schemes have been proposed. In those schemes, either ARMA model or linear state space model was used for the control law design, but ignoring the nonlinear coupling effects.

Recently, the perturbation technique has attracted widespread attention. Using the technique, the dynamics of a flexible robot can be decomposed into two subsystems, namely, a slow subsystem and a fast subsystem. The slow subsystem corresponds to the rigid body movement and the fast subsystem is mainly to account for the elastic modes. Usually, the composite control schemes are designed to deal with this kind of formulation. ([12], [13])

Seeing et al. [9]-[11], used the so-called input-preshaping technique, which applied a set of impulse train to convolve with the input command so as to suppress the vibration modes. Some researchers [14]-[15] used the fuzzy control methodolgy for the control of flexible arm.

In [7], [8], several nonlinear control schemes, such as computed torque, inverse dynamics, and feedback linearization, have been proposed for the control of multilink flexible robot arms, but the elastic part was always ignored. In the recent work by Yang et al.[16], a generalized computed torque control with elastic regulation was proposed. In this paper, the method is extended to an adaptive control which enables one to handle parametric uncertainties.

One should note that most of the proposed control strategies, which used the flexible modes as feedback signals, may be inconvenient for practical implementation since the flexible modes can only be obtained by some on-line calculation which is very time-consuming and mode-shape-dependent. So, in this paper, the flexible-mode-dependent dynamics is first formulated into a strain-dependent one, based on which an adaptive variable structure scheme is then proposed to reduce the computational burden due to full parameter adaptation [16]. To alleviate the chattering caused by switching, a saturation type adaptive control is also presented.

This paper is organized as follows: Section 2 formulates the conventionally used model into a strain dependent one. In Section 3, an adaptive variable structure control is designed for a general flexible robot arm. To alleviate the chattering, an alternative control of saturation type is then proposed in Section 4. In Section 5, some simulation results are shown to demonstrate the control performance. Finally, concluding remarks are given in Section 6.

2 Dynamic Formulation

Consider an n-link flexible manipulator with m flexible modes having the following dynamics:

$$M(q)\ddot{q} + C(q,\dot{q})\dot{q} + K_m q = Q\tau \tag{1}$$

IEEE International Conference
on Robotics and Automation
0-7803-1965-6/95 $4.00 ©1995 IEEE

where $Q = \begin{bmatrix} I \\ 0 \end{bmatrix}$, $q = \begin{bmatrix} q_r \\ q_f \end{bmatrix}$ represents the joint angles and flexible modes, respectively and τ is the generalized torque (force) of the manipulator system at each joint. It is noteworthy that in physical implementation the true measured information are the strain signals rather than the magnitude of the vibration modes, q_f, and hence some transformation should be done to reformulate the system dynamics into a output-feedback form. Let the strain measurement at some location l of link i be $y_i(l,t)$, then

$$y_i(l,t) = \frac{d_i}{2}\sum_{j=1}^{m_i} \frac{d^2}{dx^2}\phi_j(x)\Big|_{x=l} q_{f_{ij}}(t)$$

where

- d_i : thickness of link i
- $\phi_j(x)$: the jth mode-shape function of link i
- $q_{f_{ij}}(t)$: the jth flexible mode of link i
- m_i : number of flexible modes assumed in link i

and if we attach m_i strain gauges along the ith link at different locations, namely, $x_1, x_2, \cdots, x_{m_i}$, then

$$y_i = \Psi_i q_{f_i}(t) \tag{2}$$

where $y_i = [y_i(x_1,t), \cdots, y_i(x_{m_i},t]^T$ and

$$\Psi_i = \frac{d_i}{2}\begin{bmatrix} \frac{d^2}{dx^2}\phi_1(x_1) & \cdots & \frac{d^2}{dx^2}\phi_{m_i}(x_1) \\ \vdots & \ddots & \vdots \\ \frac{d^2}{dx^2}\phi_1(x_{m_i}) & \cdots & \frac{d^2}{dx^2}\phi_{m_i}(x_{m_i}) \end{bmatrix}$$

It should noted that as long as the locations of the strain gauges $x_1, x_2, \cdots, x_{m_i}$ are fixed, Ψ_i is a constant matrix. we can then group the strain measurements for all the links to yield

$$y \equiv \begin{bmatrix} y_1 \\ \vdots \\ y_n \end{bmatrix} = diag[\Psi_1, \Psi_2, \cdots, \Psi_n]\begin{bmatrix} q_{f_1} \\ \vdots \\ q_{f_n} \end{bmatrix} \equiv \Psi q_f$$

so that the signal vector q_f can be replaced by the strain information y as follows:

$$q_f = \Psi^{-1} y$$

provided Ψ_i was made nonsingular, and so is Ψ by appropriately choosing the strain gauge locations. Therefore, the dynamic equations (1) become

$$M\Omega\begin{bmatrix} \ddot{q}_r \\ \ddot{y} \end{bmatrix} + C\Omega\begin{bmatrix} \dot{q}_r \\ \dot{y} \end{bmatrix} + K_m\Omega\begin{bmatrix} q_f \\ y \end{bmatrix} = \begin{bmatrix} \tau \\ 0 \end{bmatrix} \tag{3}$$

where

$$\Omega = \begin{bmatrix} I & 0 \\ 0 & \Psi^{-1} \end{bmatrix}$$

If we multiply both sides by Ω^T, then the following equation can be obtained

$$\bar{M}\begin{bmatrix} \ddot{q}_r \\ \ddot{y} \end{bmatrix} + \bar{C}\begin{bmatrix} \dot{q}_r \\ \dot{y} \end{bmatrix} + \bar{K}_m\begin{bmatrix} q_r \\ y \end{bmatrix} = \begin{bmatrix} \tau \\ 0 \end{bmatrix} \tag{4}$$

where $\bar{M} = \Omega^T M\Omega$, $\bar{C} = \Omega^T C\Omega$, and $\bar{K}_m = \Omega^T K_m\Omega$. In the subsequent section, the equations derived above will be valid for the strain-feedback controller design.

Remarks :

(1) In the above formulation, it is required that Ψ should be nonsingular. Generally, this condition can be easily satisfied by properly designing the locations of strain gauges.

(2) One can always find a C matrix such that $x^T(\dot{M} - 2C)x = 0$, $\forall x \in R^n$, and the same result will hold for $\bar{M}$, $\bar{C}$, since $x^T(\dot{\bar{M}} - 2\bar{C})x = x^T\Omega^T(\dot{M} - 2C)\Omega x = (\Omega x)^T(\dot{M} - 2C)(\Omega x) = 0$, $\forall x \in R^n$

3 Adaptive Variable Structure Design

Consider equation (4) and partition the inertia and Coriolis matrices into four sub-matrices corresponding to the rigid and flexible parts, respectively, namely,

$$\begin{bmatrix} m_{rr} & m_{rf} \\ m_{fr} & m_{ff} \end{bmatrix}\begin{bmatrix} \ddot{q}_r \\ \ddot{y} \end{bmatrix} + \begin{bmatrix} c_{rr} & c_{rf} \\ c_{fr} & c_{ff} \end{bmatrix}\begin{bmatrix} \dot{q}_r \\ \dot{y} \end{bmatrix} + \begin{bmatrix} 0 & 0 \\ 0 & k_F \end{bmatrix}\begin{bmatrix} q_r \\ y \end{bmatrix} = \begin{bmatrix} \tau \\ 0 \end{bmatrix} \tag{5}$$

Let $q_{rd}(t)$, $\dot{q}_{rd}(t)$, $\ddot{q}_{rd}(t)$ denote the desired trajectory, its first- and second-order derivatives, respectively, and define the sliding surface as follows:

$$s = \begin{bmatrix} s_r \\ s_f \end{bmatrix} = \begin{bmatrix} \dot{e}_r + \lambda_r e_r \\ \dot{y} + \lambda_f y \end{bmatrix} = \dot{e} + \lambda e$$

where $e = [e_r, y]^T$, $\lambda = diag[\lambda_r, \lambda_f] > 0$ and $e_r = q_r - q_{rd}$ is the error signals for joint angles. After some proper manipulation, the dynamics of the newly defined system with respect to s_r, s_f can be derived as :

$$\bar{M}\dot{s} + \bar{C}s + \bar{K}s = \begin{bmatrix} \tau + v_r + k_{vr}s_r \\ v_f \end{bmatrix} \tag{6}$$

where

$$\begin{aligned} v_r &= m_{rr}(-\ddot{q}_{rd} + \lambda_r\dot{e}_r) + m_{rf}(\lambda_f\dot{y}) \\ &\quad + c_{rr}(-\dot{q}_{rd} + \lambda_r e_r) + c_{rf}(\lambda_f y) \\ v_f &= mfr(-\ddot{q}_{rd} + \lambda_r\dot{e}_r) + m_{ff}(\lambda_f\dot{y}) \\ &\quad + c_{fr}(-\dot{q}_{rd} + \lambda_r e_r) + c_{ff}(\lambda_f y) + k_{vf}s_f - k_F y \\ \bar{K} &= \begin{bmatrix} k_{vr} & 0 \\ 0 & k_{vf} \end{bmatrix} \end{aligned}$$

and k_{vr}, k_{vf} are some positive definite constant matrices.

Remark:

It can be easily verified that v_r and v_f preserve the linear-in-parameter property, i.e,

$$\begin{aligned} v_r &= W_r(q_r, \dot{q}_r, y, \dot{y}, t)\theta_r \\ v_f &= W_f(q_r, \dot{q}_r, y, \dot{y}, t)\theta_f \end{aligned}$$

where W_r, W_f represent the regressor matrices which contain all the known functions, and θ_r, θ_f consist of the unknown constant parameters. Furthermore, $\|\theta_r\|$, $\|\theta_f\|$ are bounded by some positive constants α_1, α_2, respectively, i.e.,

$$\|v_r\| \leq \|W_r\|\|\theta_r\| \leq \|W_r\|\alpha_1 \quad (7)$$

$$\|v_f\| \leq \|W_f\|\|\theta_f\| \leq \|W_f\|\alpha_2 \quad (8)$$

Now, let the proposed control law be

$$\begin{aligned} \tau &= -k_{vr}s_r - \tau_c \quad (9) \\ \tau_c &= sign(s_r)\|W_r\|\hat{\alpha_1} + \frac{(1+k)s_r}{\|s_r\|^2+\epsilon}(\|s_f\|\|W_f\|\hat{\alpha_2}) \end{aligned}$$

with the adaptation law $\hat{\alpha_1}$, $\hat{\alpha_2}$, and k satisfying

$$\dot{\hat{\alpha_1}} = \frac{1}{k_1}\|W_r\|\|s_r\| \quad (10)$$

$$\dot{\hat{\alpha_2}} = \frac{1}{k_2}\|W_f\|\|s_f\| \quad (11)$$

$$\dot{k} = \begin{cases} \frac{1}{k}\left(\frac{k\|s_r\|^2-\epsilon}{\|s_r\|^2+\epsilon}\right)(\|s_f\|\|W_f\|\hat{\alpha_2}) & , k \neq 0 \\ \delta & , k = 0 \end{cases} \quad (12)$$

for some k_1, k_2, where $\hat{\alpha_1}$, $\hat{\alpha_2}$ are the estimates of α_1 and α_2, respectively, and ϵ and δ are some small positive constants. It can be shown that the error dynamics resulting from the above control laws (9)-(12) are asymptotically stable in the sense of Lyapunov, and the details will be stated in the following theorem.

Theorem 1 *Consider a multilink flexible manipulator with dynamic model being described by (5) or (6). Let the control objective be to force the joints to follow some prespecified trajectories, while simultaneously damping out the vibrational modes. Then, the proposed control laws can achieve this objective asymptotically, i.e.,* $e \to 0$ *and* $y \to 0$ *asymptotically as* $t \to \infty$.

Proof:
Consider the Lyapunov function candidate

$$V = \frac{1}{2}s^T\bar{M}s + \frac{1}{2}k_1\tilde{\alpha}_1^2 + \frac{1}{2}k_2\tilde{\alpha}_2^2 + \frac{1}{2}k^2 \quad (13)$$

where

$$\begin{aligned} \tilde{\alpha}_1 &= \hat{\alpha_1} - \alpha_1 \\ \tilde{\alpha}_2 &= \hat{\alpha_2} - \alpha_2 \end{aligned}$$

and take the time derivative of $V(t)$ along the dynamics (6) to obtain

$$\begin{aligned} \frac{d}{dt}V &= s^T\bar{M}\dot{s} + \frac{1}{2}s^T\dot{\bar{M}}s + k_1\tilde{\alpha}_1\dot{\tilde{\alpha}}_1 + k_2\tilde{\alpha}_2\dot{\tilde{\alpha}}_2 + k\dot{k} \\ &= s^T(-\bar{C}s - \bar{K}s + \begin{bmatrix} \tau + v_r + k_{vr}s_r \\ v_f \end{bmatrix}) \\ &\quad + \frac{1}{2}s^T\dot{\bar{M}}s + k_1\tilde{\alpha}_1\dot{\tilde{\alpha}}_1 + k_2\tilde{\alpha}_2\dot{\tilde{\alpha}}_2 + k\dot{k} \\ &= -s^T\bar{K}s + s_r^T(\tau + v_r + k_{vr}s_r) + s_f^Tv_f \\ &\quad + k_1\tilde{\alpha}_1\dot{\tilde{\alpha}}_1 + k_2\tilde{\alpha}_2\dot{\tilde{\alpha}}_2 + k\dot{k} \\ &\leq -s^T\bar{K}s + s_r^T\tau + \|s_r\|\|v_r\| + s_r^Tk_{vr}s_r \\ &\quad + \|s_f\|\|v_f\| + k_1\tilde{\alpha}_1\dot{\tilde{\alpha}}_1 + k_2\tilde{\alpha}_2\dot{\tilde{\alpha}}_2 + k\dot{k} \\ &\leq -s^T\bar{K}s + s_r^T\tau + \|s_r\|\|W_r\|\alpha_1 + s_r^Tk_{vr}s_r \\ &\quad + \|s_f\|\|W_f\|\alpha_2 + k_1\tilde{\alpha}_1\dot{\tilde{\alpha}}_1 + k_2\tilde{\alpha}_2\dot{\tilde{\alpha}}_2 + k\dot{k} \end{aligned}$$

If we substitute the developed control laws (9)-(12) into the above equation, we can obtain the following inequality

$$\begin{aligned} \dot{V} &\leq -s^T\bar{K}s + \|s_r\|\|W_r\|(\alpha_1 - \hat{\alpha_1}) \\ &\quad - \frac{(1+k)\|s_r\|^2}{\|s_r\|^2+\epsilon}(\|s_f\|\|W_f\|\hat{\alpha_2}) \\ &\quad + \|s_f\|\|W_f\|\alpha_2 + k_1\dot{\hat{\alpha_1}}\tilde{\alpha_1} + k_2\dot{\hat{\alpha_2}}\tilde{\alpha_2} + k\dot{k} \\ &\leq -s^T\bar{K}s - \frac{k\|s_r\|^2}{\|s_r\|^2+\epsilon}(\|s_f\|\|W_f\|\hat{\alpha_2}) \\ &\quad + \frac{\epsilon}{\|s_r\|^2+\epsilon}(\|s_f\|\|W_f\|\hat{\alpha_2}) + k\dot{k} \\ &\leq -s^T\bar{K}s \qquad when \qquad k \neq 0 \end{aligned}$$

Since $V(t)$ is a continuous function of k, $V(t)$ is noincreasing in t, which implies the boundedness of s, $\hat{\alpha_1}$, $\hat{\alpha_2}$, and k, and in turn the boundedness of $\dot{s}$, q_r, and y or q_f. Then, by Barbalat's lemma [17], we can conclude that

$$s \to 0 \qquad as \qquad t \to \infty \qquad asymptotically$$

which implies

$$e,\ \dot{e} \to 0 \qquad as \qquad t \to \infty \qquad asymptotically$$

This completes our proof. Q.E.D.

Remark:

(1) One should note that the proposed adaptation law (12) contains $\frac{1}{k}$ which may be no longer feasible as $k(t)$ is equal to zero. As a consequence, the value of $k(t)$ will be projected away from zero when $k(t)$ is equal to zero so that the well-posedness of $k(t)$ is guaranteed. In addition, the initial condition of k may be chosen sufficiently large, i.e.,

$$k(0) >> \frac{\epsilon}{\|s_r(0)\|^2}$$

for practical implementation.

(2) In theory, ϵ can be chosen to be arbitrary positive value. However, in practice, the larger ϵ is, the slower the convergence rate of s will be, and hence, e_r and y.

4 Adaptive Saturation Type Controller Design

In this section, a saturation-function term is proposed in place of the $sign(s_r)$ to alleviate the chattering phenomenon due to the switching mechanism in the previous controller (9).

For convenience, let us re-consider the s-dependent dynamics (6) and let the control laws be redesigned as :

$$\begin{aligned} \tau &= -k_{vr}s_r - \hat{\alpha}_1\|W_r\|sat(\frac{\hat{\alpha}_1\|W_r\|s_r}{\mu}) \\ &\quad - \frac{(1+k)s_r}{[illegible]}(\hat{\alpha}_2\|W_f\|\|s_f\|) \quad (14) \end{aligned}$$

with $\hat{\alpha_1}$, $\hat{\alpha_2}$, and k satisfying

$$\dot{\hat{\alpha}}_1 = \frac{1}{k_1}[\|s_r\|\|W_r\| - \sigma_1(\hat{\alpha}_1 - \alpha_1^*)] \tag{15}$$

$$\dot{\hat{\alpha}}_2 = \frac{1}{k_2}[\|s_f\|\|W_f\| - \sigma_2(\hat{\alpha}_2 - \alpha_2^*)] \tag{16}$$

$$\dot{k} = \begin{cases} \frac{p}{k}\left(\frac{k\|s_r\|^2-\epsilon}{\|s_r\|^2+\epsilon}\right)(\|s_f\|\|W_f\|\hat{\alpha_2}) - p\sigma_3 k & , k \neq 0 \\ \delta & , k = 0 \end{cases} \tag{17}$$

where p is some positive constant and $sat(x) = [sat(x_1)\cdots sat(x_n)]^T$ with

$$sat(x_i) = \begin{cases} x_i & \|x\| \leq 1 \\ sgn(x_i) & \|x\| > 1 \end{cases} \qquad i = 1, 2, \cdots, n$$

and μ is some positive constant, σ_1, σ_2, $\sigma_3 > 0$, and furthermore, α_1^*, $\alpha_2^* > 0$ are some designed parameters. In the following, it is shown that all the signals of the system dynamics along with the control laws (14)-(17) are ultimately bounded. This will be precisely stated in the following theorem.

Theorem 2 *Consider the same system as described in Theorem 1. Then, by applying the control laws (17)-(20), the error vectors e, y will be driven into in a residual set with size $O(\delta)$ exponentially in time t, where $\delta = \mu + \frac{1}{2}[\sigma_1(\alpha_1 - \alpha_1^*)^2 + \sigma_2(\alpha_2 - \alpha_2^*)^2]$.*

Proof:

Choose a Lyapunov function candidate as

$$V = \frac{1}{2}s^T\bar{M}s + \frac{1}{2}k_1\tilde{\alpha}_1^2 + \frac{1}{2}k_2\tilde{\alpha}_2^2 + \frac{1}{2}p^{-1}k^2 \tag{18}$$

where $\tilde{\alpha}_1 = \hat{\alpha}_1 - \alpha_1$, $\tilde{\alpha}_2 = \hat{\alpha}_2 - \alpha_2$ are the parameter estimation errors. Obviously, the chosen Lyapunov function candidate can be upper bounded by some quadratic function as

$$V \leq \lambda_1 X^T X$$

where

$$X^T = [s^T, \tilde{\alpha}_1, \tilde{\alpha}_2, k]^T$$
$$\lambda_1 = \frac{1}{2}max(\lambda_{max}(\bar{M}), k_1, k_2, p^{-1})$$

and $\lambda_{max}(z)$ denotes the maximum eigenvalue of z. Then the time derivative of the Lyapunov function along dynamics (6) can be derived as :

$$\begin{aligned} \dot{V} &= s^T\bar{M}\dot{s} + \frac{1}{2}s^T\dot{\bar{M}}s + k_1\tilde{\alpha}_1\dot{\tilde{\alpha}}_1 + k_2\tilde{\alpha}_2\dot{\tilde{\alpha}}_2 + p^{-1}k\dot{k} \\ &= s^T(-\bar{C}s - \bar{K}s + \begin{bmatrix} \tau + k_{vr}s_r + v_r \\ v_f \end{bmatrix}) \\ &\quad + \frac{1}{2}s^T\dot{\bar{M}}s + k_1\tilde{\alpha}_1\dot{\tilde{\alpha}}_1 + k_2\tilde{\alpha}_2\dot{\tilde{\alpha}}_2 + p^{-1}k\dot{k} \\ &= -s^T\bar{K}s + s_r^T\tau + s_rk_{vr}s_r + s_r^Tv_r \\ &\quad + s_f^Tv_f + k_1\tilde{\alpha}_1\dot{\tilde{\alpha}}_1 + k_2\tilde{\alpha}_2\dot{\tilde{\alpha}}_2 + p^{-1}k\dot{k} \end{aligned}$$

If the control laws (14)-(17) are applied, then

$$\begin{aligned} \dot{V} &\leq -s^T\bar{K}s - s_r^T\hat{\alpha}_1\|W_r\|sat(\frac{\hat{\alpha}_1\|W_r\|s_r}{\mu}) + \alpha_1\|s_r\|\|W_r\| \\ &\quad - \frac{(1+k)\|s_r\|^2}{\|s_r\|^2+\epsilon}(\|s_f\|\|W_f\|\hat{\alpha_2}) + \alpha_2\|s_f\|\|W_f\| \\ &\quad + \tilde{\alpha}_1\|W_r\|\|s_r\| + \tilde{\alpha}_2\|W_f\|\|s_f\| - \mu \\ &\quad + \frac{k\|s_r\|^2-\epsilon}{\|s_r\|^2+\epsilon}(\|s_f\|\|W_f\|\hat{\alpha_2}) \\ &\quad - \sigma_1\tilde{\alpha}_1(\hat{\alpha}_1 - \alpha_1^*) - \sigma_2\tilde{\alpha}_2(\hat{\alpha}_2 - \alpha_2^*) - \sigma_3k^2 \\ &\leq -s^T\bar{K}s - s_r^T\hat{\alpha}_1\|W_r\|sat(\frac{\hat{\alpha}_1\|W_r\|s_r}{\mu}) + \hat{\alpha}_1\|W_r\|\|s_r\| \\ &\quad - \sigma_1\tilde{\alpha}_1(\hat{\alpha}_1 - \alpha_1^*) - \sigma_2\tilde{\alpha}_2(\hat{\alpha}_2 - \alpha_2^*) - \sigma_3k^2 \end{aligned} \tag{19}$$

By completing the square, it can be shown that

$$\begin{aligned} -\sigma_1\tilde{\alpha}_1(\hat{\alpha}_1 - \alpha_1^*) &= -\sigma_1\tilde{\alpha}_1(\hat{\alpha}_1 - \alpha_1 + \alpha_1 - \alpha_1^*) \\ &= -\sigma_1\tilde{\alpha}_1^2 - \sigma_1\tilde{\alpha}_1(\alpha_1 - \alpha_1^*) \\ &\leq -\frac{1}{2}\sigma_1\tilde{\alpha}_1^2 + \frac{1}{2}\sigma_1(\alpha_1 - \alpha_1^*)^2 \end{aligned}$$

and similarly,

$$-\sigma_2\tilde{\alpha}_2(\hat{\alpha}_2 - \alpha_2^*) \leq -\frac{1}{2}\sigma_2\tilde{\alpha}_2^2 + \frac{1}{2}\sigma_2(\alpha_2 - \alpha_2^*)^2,$$

so that equation (19) becomes

$$\begin{aligned} \dot{V} &\leq -s^T\bar{K}s - \frac{1}{2}\sigma_1\tilde{\alpha}_1^2 - \frac{1}{2}\sigma_2\tilde{\alpha}_2^2 + \hat{\alpha}_1\|W_r\|\|s_r\| \\ &\quad - s_r^T\hat{\alpha}_1\|W_r\|sat(\frac{\hat{\alpha}_1\|W_r\|s_r}{\mu}) + \gamma \end{aligned} \tag{20}$$

where

$$\gamma = \frac{1}{2}[\sigma_1(\alpha_1 - \alpha_1^*)^2 + \sigma_2(\alpha_2 - \alpha_2^*)^2]$$

In the following, two cases are analyzed to evaluate the stability of the overall system.

(I) $\hat{\alpha}_1\|W_r\|\|s_r\| > \mu$

Since $\hat{\alpha}_1(t)$ must be a positive function as shown in (15), $\hat{\alpha}_1(t) \geq 0$ if $\hat{\alpha}_1(0) \geq 0$. Therefore,

$$sat(\frac{\hat{\alpha}_1\|W_r\|s_r}{\mu}) = sign(s_r)$$

and, hence, (20) becomes

$$\begin{aligned} \dot{V} &\leq -s^T\bar{K}s - \frac{1}{2}(\sigma_1\tilde{\alpha}_1^2 + \sigma_2\tilde{\alpha}_2^2) - \sigma_3k^2 + \gamma \\ &\leq -\frac{\lambda_2}{\lambda_1}V + \gamma \end{aligned}$$

where $\lambda_2 = min(\lambda_{min}(\bar{K}), \frac{1}{2}\sigma_1, \frac{1}{2}\sigma_2, \sigma_3)$.

(II) $\hat{\alpha}_1\|W_r\|\|s_r\| \leq \mu$

In this case,

$$sat(\frac{\hat{\alpha}_1\|W_r\|s_r}{\mu}) = \frac{\hat{\alpha}_1\|W_r\|s_r}{\mu} \tag{21}$$

and we will have the following inequality from (20)

$$\begin{aligned} \dot{V} &\leq -s^T\bar{K}s - \frac{1}{2}(\sigma_1\tilde{\alpha}_1^2 + \sigma_2\tilde{\alpha}_2^2) - \sigma_3k^2 + \gamma \\ &\quad - \hat{\alpha}_1\|W_r\|\|s_r\|\left[\frac{\hat{\alpha}_1\|W_r\|\|s_r\|}{\mu} - 1\right] \\ &\leq -\frac{\lambda_2}{\lambda_1}V + \delta \end{aligned}$$

where we have used the fact that $-1 \leq \frac{\hat{\alpha}_1 \|W_r\| \|s_r\|}{\mu} - 1 \leq 0$. From the two cases shown above, we can conclude that $\|s\|$ will eventually fall into a residual set with size $O(\gamma + \mu)$, and so will $\|e\|$ and $\|y\|$. This concludes our proof. Q.E.D.

Remark :

The constant parameters α_1^* and α_2^* can be designed to be some values satisfying $0 \leq \alpha_1^* \leq 2\alpha_1$ and $0 \leq \alpha_2^* \leq 2\alpha_2$, respectively. Clearly, the addition of α_1^* and α_2^* in the adaptation law will lead to a better result than the conventional σ-modification scheme in which $\alpha_1^* = \alpha_2^* = 0$. Besides, the closer α_i^* is to α_i, $i = 1, 2$, the smaller γ becomes. For practical implementation , α_1^* and α_2^* may be chosen according to the prior knowledge of α_1 and α_2, respectively, or by some trials and errors.

5 Experimental Verification

5.1 Apparatus

In this section, some experimental results of these two types of controller are shown. A two-link flexible manipulator has been designed and experimented in the Department of Electrical Engineering, National Taiwan University (NTU), as shown in Fig.(1). The two-link flexible arm is a planar type robot with revolute joints which are perpendicular to the motional plane. The motor mounted on the second joint of this robot arm is air-supported in order to counteract the gravitation effects. The mathematical model of this arm is derived based on the assumed-mode approach by using *Mathematica* [18] software package. The parameters of this manipulator are listed below :

- length of the 1st link : 0.4 m
- length of the 2nd link : 0.5 m
- thickness of the 1st link : 2 mm
- thickness of the 2nd link : 1 mm
- flexural rigidity of the 1st link : 3.677 Nm^2
- flexural rigidity of the 2nd link : 0.46 Nm^2
- weight of the hub mounted on the 2nd joint : 3.21 kg

Both links are made of Aluminum (6061-T6). The first link is driven by a D.C. motor with gear down ratio 128:1 and the second link is driven by a D.C. brushless motor with gear down ratio 100:1. An optical encoder is embedded in each motor for the measurements of angular position. The velocities of motor shafts are then obtained by the differentiation of angular position through some properly designed low-pass filter. Besides, to account for the torsional effects due to the gravitational force, an air-jet device is attached to the bottom of the second joint. Moreover, the link deflections are measured by strain gauges, two for each link. Also, the high frequency modes are filtered by some properly designed low-pass filter to alleviate the spillover problem. In addition, the PC-486-33 is used as the processor for implementing the proposed control law, and the sampling rate is chosen to be 500 Hz.

5.2 Results

In the experiment of saturation type of control, the control parameters are chosen as $\lambda_r = diag[1.5, 1.5]$, $\lambda_f = diag[1.2, 1.2, 1.2, 1.2]$, $k_{vr} = diag[1.2, 1.5]$, $k_{vf} = diag[1.5, 1.5, 1.5, 1.5]$, $k_1 = k_2 = 0.5$, $\epsilon = 0.1$, and μ is chosen as 0.01. The desired trajectories for both joints are

$$q_{1d} = \frac{\pi}{4}(6(\frac{t}{T_m})^5 - 15(\frac{t}{T_m})^4 + 10(\frac{t}{T_m})^3)(rad)$$
$$q_{2d} = \frac{\pi}{4}(6(\frac{t}{T_m})^5 - 15(\frac{t}{T_m})^4 + 10(\frac{t}{T_m})^3)(rad)$$

where $T_m = 3\ sec$ is the expected duration of motion. The experimental results are plotted in Fig.(2)-Fig.(5). Fig.(2)-Fig.(3) show the trajectories of the rigid parts whereas Fig.(4)-Fig(5) show the trajectories of the strain signal of each link.

6 Conclusion

In this paper, two adaptive robust control approaches, which directly use strain measurements instead of elastic-mode information, have been proposed for the control of flexible manipulators. The first approach is an adaptive variable structure type of scheme which can massively reduce the computational complexity commonly deserved in the fully adaptive scheme, but it will work at the price of chattering. To avoid this problem, a saturation type of adaptive control law is then developed to alleviate such undesirable phenomenon. Experimental results are also shown to verify the effectiveness of the controller.

References

[1] Robert H. Cannon and Jr. Eric Schmitz, "Initial Experiments on the End-Point Control of a Flexible One-Link Robot, " Int. J. of Robotics Research, Vol. 3, No. 3, pp. 62-75, Fall 1984.

[2] I.Y. Shung and M. Vidyasagar, "Control of a Flexible Robot Arm with Bounded Input: Optimum Step Response," IEEE Int. Conf. on Robotics and Automation, pp. 916-922, 1987.

[3] D. Nemier, A.J. Koivo, and R.L. Kashyap, "Control of Gripper Position of a Compliant Link Using Strain Gauge Measurements," IEEE, Conf. on Decision and Control, pp. 1140-1144, Dec. 1986.

[4] J.-S. Chen and C.-H. Menq, " Modeling and Adaptive Control of a Flexible One-Link Manipulator, " Robotica, Vol. 8, pp. 339-345, 1990.

[5] Ümit Özgüner, Stephen Yurkovich, Joseph W. Martin, and Paul T. Kotnik, " Laboratory Facility for Flexible Structure Control Experiments, " IEEE Control Systems Mag., pp. 27-33, Aug. 1988.

[6] Paul T. Kotnik, Stephen Yurkovich and Ümit Özgüner, Stephen Yurkovich," Acceleration Feedback for Control of a Flexible Manipulator Arm, " J. of Robotic Systems, pp. 181-195, May 1988.

[7] C. M. Pham, W. Khalil, and C. Chevallereau, " A Nonlinear Model-Based Control of Flexible Robots, " Robotica, Vol. 11, pp. 73-82, April 1992.

[8] Wayne J. Book, "Recursive Lagrangian Dynamics of Flexible Manipulator Arms," Int. J. of Robotics Research, Vol. 3, No. 3, pp. 87-101, Fall 1984.

[9] J.M. Hyde and W.P. Seering, " Using Input Command Pre-Shapping to Suppress Multiple Mode Vibration, " Proc. IEEE Conf. on Robotics and Automation, pp. 2604-2610, April 1991.

[10] David P. Magee and Wayne J. Book, " Eliminating Multiple Modes of Vibration in a Flexible Manipulator, " Proc. IEEE Conf. on Robotics and Automation, pp. 474-479, 1993.

[11] T. Singh and G.R. Heppler, " Shaped Inputs for a multimode System, " Proc. IEEE Conf. on Robotics and Automation, pp. 474-479, 1993.

[12] B. Siciliano and W. J. Book, "A Singular Perturbation Approach to control of lightweight flexible manipulators", Int. J. Robotics Research, Vol. 7, No. 4, Aug. 1988.

[13] F.L. Lewis and M. Vandegrift, " Flexible Robot Arm Control by a Feedback Linearization-Singular Perturbation Approach, " Proc. IEEE Conf. on Robotics and Automation, pp. 474-479, 1993.

[14] E. Garacia-Benitez, Stephen Yurkovich, and Kevin M. Passino, " Rule-Based Supervisory Control of a Two-Link Flexible Manipulator, " J. of Intelligent and Robotic Systems, pp. 195-213, 1993.

[15] Eric Kubica and David Wang, " A Fuzzy Control Strategy for a Flexible Single Link Robot, " Proc. IEEE Conf. on Robotics and Automation, pp. 236-241, 1993.

[16] J. H. Yang, F. C. Liu, and L. C. Fu, "Nonlinear Control for Flexible Manipulators", Proc. of Conf. on Robotics and Automation, 1994.

[17] V. M. Popov, "Hyperstability of Control Systems", New York : Spring-Verlag, 1973.

[18] S. Wolfram, "Mathematica, A System for Doing Mathematics by Computer", Addison-Wesley Publishing Company, 1988.

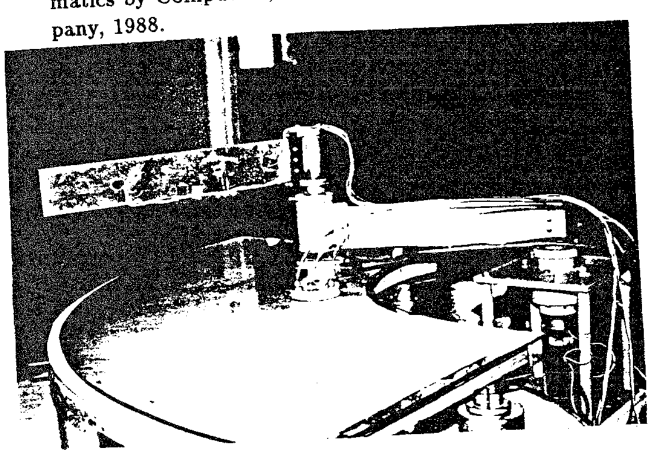

Fig.(1) Experimental Setup of the 2-link Flexible Arm

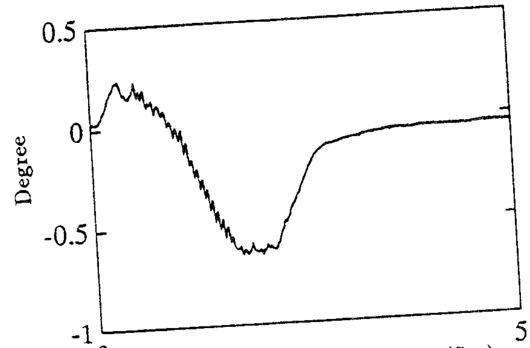

Fig.(2) Joint 1 Tracking Error(Sec)

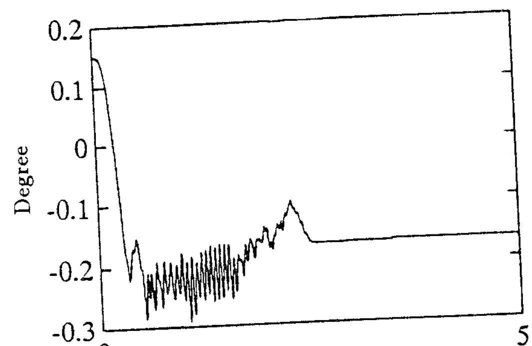

Fig.(3) Joint 2 Tracking Error(Sec)

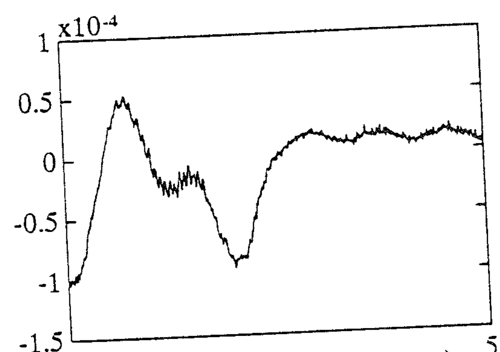

Fig.(4) Strain Signal of Link 1(Sec)

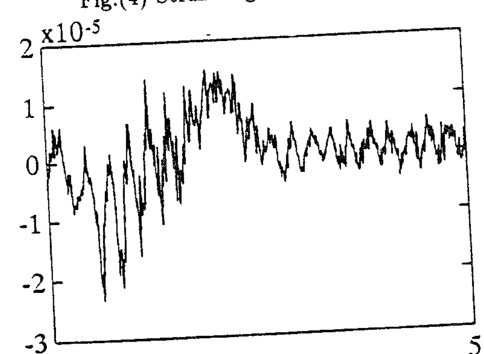

Fig.(5) Strain Signal of Link 2(Sec)